Dyes and Pigments 86 (2010) 97–105

Contents lists available at ScienceDirect

Dyes and Pigments

journal homepage: www.elsevier.com/locate/dyepig

The synthesis, spectroscopic characterization and structure of three bis(arylmethylidene)cyclopentanones

Yi-Feng Sun [a,b,*], Zhu-Yuan Wang [b], Xue Zhao [a], Ze-Bao Zheng [a], Ji-Kun Li [a], Ren-Tao Wu [a], Yi-Ping Cui [b]

[a] *Department of Chemistry, Taishan University, Taian 271021, China*
[b] *Advanced Photonics Center, School of Electronic Science and Engineering, Southeast University, Nanjing 210096, China*

ARTICLE INFO

Article history:
Received 2 November 2009
Received in revised form
7 December 2009
Accepted 10 December 2009
Available online 4 January 2010

Keywords:
Bis(arylmethylidene)cycloalkanone
Spectroscopy
Crystal structure
Density function theory
Frontier orbital
Quantum chemical calculations

ABSTRACT

Three bis(arylmethylidene)cyclopentanone dyes were synthesized and their structures and properties elucidated using single-crystal X-ray diffraction, mass spectrometry, ^{1}H nuclear magnetic resonance, IR and UV–Vis spectroscopy. X-ray analyses revealed that two were monoclinic, with space group $P2_1/c$, while the third dye was triclinic, with space group $P\bar{1}$. All three molecules adopted an *E*-configuration about the central olefinic bonds, exhibiting a butterfly-shaped geometry. Molecular structure optimization using density function theory revealed that the optimized geometer parameters were in reasonably good agreement with experimental values. In addition, the highest occupied molecular orbital and lowest unoccupied molecular orbital levels were deduced.

© 2009 Elsevier Ltd. All rights reserved.

1. Introduction

The bis(arylmethylidene)cycloalkanone moiety is both a novel pharmacophore and an important chromophore. Molecules that comprise such a structural unit are of special interest owing to their broad spectrum of activities and applications. Curcumin (Fig. 1) is a naturally occurring yellow pigment isolated from the root of *Curcuma longa* rhizomes, and exhibits a wide range of biological activities [1–5]. As a class of conjugated monoketone analogues of Curcumin, the bis(arylmethylidene)cycloalkanones have been already reported to posses potential anti-HIV protease activity, cytotoxic, cancer chemopreventive and antioxidant properties [6–14]. Furthermore, these compounds are more compact than Curcumin and are readily synthesized. Recent, it has been reported that some compounds containing the 3-(3,4,5-trimethoxyphenyl)-2-propenoyl group displayed potent multidrug resistance (MDR) reversal properties in cancer chemotherapy. In particular, 2,5-bis(3,4,5-trimethoxyphenylmethylene) cyclopentanone (**TMPCP**) (Fig. 1) was 31 times more potent than Verapamil as a MDR revertant [15].

On the other hand, some bis(arylmethylidene)cycloalkanones are found be effective photosensitive materials and fluorescent probe, and exhibit promising two-photon absorption (TPA) properties [16–19]. For example, bis(benzylidene)cyclopentanone derivatives **MPCP** and **EPCP** (Fig. 1) are well-known high-efficient sensitizing dye that is widely employed in photopolymerization systems. Also, in a very recent study it was shown that these two bis(benzylidene)cyclopentanone dyes displayed large two-photon absorption cross-sections [20,21]. Besides, bis(arylmethylidene)cycloalkanones are widely used as building blocks for the synthesis of a new class of spiro pyrrolidines as antimicrobial and antifungal agents, tricyclic thiazolo[3,2-*a*] thiapyrano[4,3-*d*] pyrimidines and related analogues as potential anti-inflammatory agents and other bioactive heterocycles [6,22,23].

As a part of our continuous interest in the synthesis, crystallography and optical evaluation of bis(arylmethylidene)cycloalkanone derivatives, three bis(arylmethylidene) cyclopentanone dyes, **1**, **2** and **3** (Fig. 2), were synthesized. Herein, we report the synthesis, crystal structure and spectroscopic characterization of these three dyes. At the same time, the molecular structures of **1** and **3** were optimized using density function theory (DFT) at B3LYP/6-31G level.

2. Experimental

2.1. Chemicals and instrument

All melting points were determined with a WRS-1A melting point apparatus and are uncorrected. Proton nuclear magnetic

---

* Corresponding author at: Department of Chemistry, Taishan University, Taian 271021, China. Tel.: +86 538 6715546; fax: +86 538 6715536.
E-mail address: sunyf50@yahoo.com.cn (Y.-F. Sun).

0143-7208/$ – see front matter © 2009 Elsevier Ltd. All rights reserved.
doi:10.1016/j.dyepig.2009.12.010

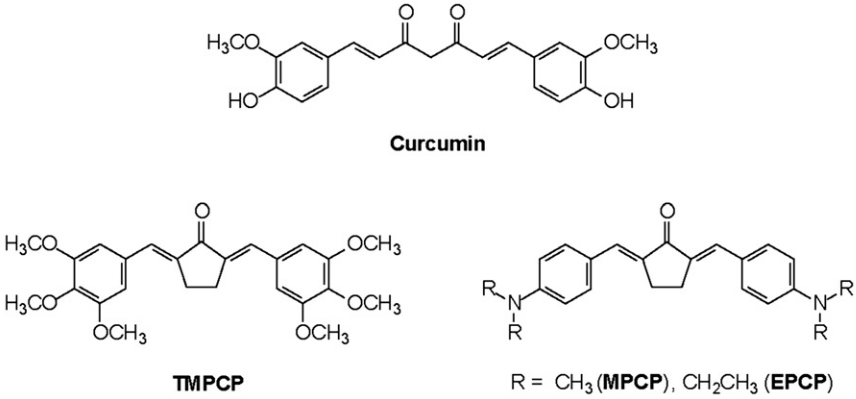

Fig. 1. The structures of Curcumin, TMPCP, MPCP and EPCP.

resonance (^{1}H NMR) spectra were run on a Bruker AV-400 or DRX-500 NMR spectrometer and chemical shifts expressed as δ (ppm) values with TMS as internal standard. IR spectra were recorded in KBr on a Nicolet NEXUS 870 FT-IR spectrophotometer. Vibrational transition frequencies are reported in wave numbers (cm^{-1}). The UV spectra were recorded using a Helios Alpha UV–Vis scanning spectrophotometer. Element analysis was taken with a Perkin–Elmer 240 analyzer. Mass spectra (MS) were measured on a LCQ Advantage MAX or VG ZAB-HS mass spectrometer. Single crystal was characterized by Enraf-Nonius CAD-4 or Bruker Smart 1000 CCD X-ray single-crystal diffractometer. All the chemicals are commercially available and they were used without further purification.

2.2. Synthesis

2.2.1. 2,5-Bis-(3-phenoxybenzylidene)cyclopentanone (1)

For the preparation of the title compound, 5 mmol of cyclopentanone and 10 mmol of 3-phenoxybenzaldehyde were dissolved in 20 mL of ethanol. To this solution, an aqueous solution (15 mL) of sodium hydroxide (75 mmol) was added dropwise with stirring at room temperature. The reaction mixture was stirred for a further 3 h and then poured into a mixture of ice and concentrated hydrochloric acid. The precipitate was filtered by suction and washed thoroughly with water and finally with ethanol. The product was dried at room temperature and crystallized from ethanol to give **1** as yellow crystals, yield 67%, mp 155–157 °C; ^{1}H NMR (400 MHz, $CDCl_3$/TMS) δ: 3.04 (s, 4H, $2 \times CH_2$), 7.03–7.08 (m, 6H, Ar-H), 7.17 (t, $J = 7.3$ Hz, 2H, Ar-H), 7.24 (t, $J = 1.8$ Hz, 2H, Ar-H), 7.32–7.44 (m, 8H, Ar-H), 7.55 (s, 2H, $2 \times {=}CH{-}$). IR (KBr) ν: 1685, 1629, 1593, 1568, 1496, 1455, 1434, 1230, 1199, 1158, 1071, 948, 892, 753, 671 cm^{-1}. MS m/z: 445 (M + 1). Anal. calcd for $C_{31}H_{24}O_3$: C 83.76, H 5.44; found: C 83.52, H 5.75.

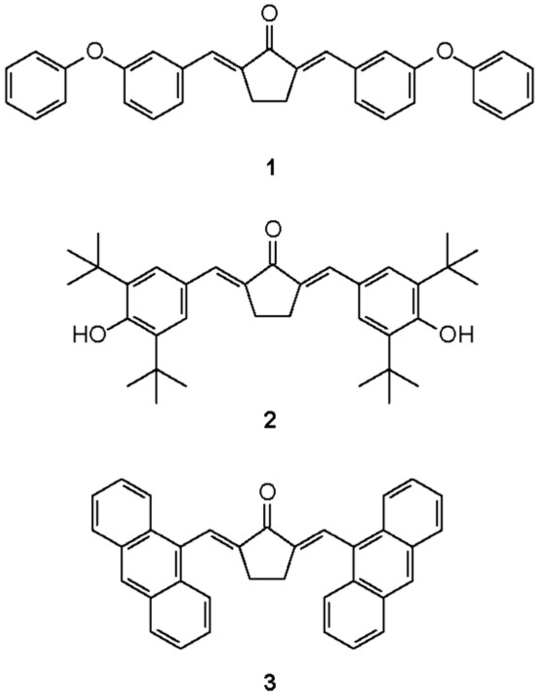

Fig. 2. The structures of bis(arylmethylidene)cyclopentanones.

2.2.2. 2,5-Bis-(3,5-di-tert-butyl-4-hydroxybenzylidene) cyclopentanone (2)

The title compound was prepared by the acid catalyzed reaction of 3,5-di-tert-butyl-4-hydroxybenzaldehyde with cyclopentanone, as previously described in [24,25] with modification. 20 mmol of 3,5-di-tert-butyl-4-hydroxybenzaldehyde and 10 mmol of cyclopentanone were dissolved in 30 mL of methanol. To this solution, 1.5 mL concentrated sulfuric acid was added dropwise with stirring at room temperature, which continued for 0.5 h. Then, the reaction mixture was refluxed for 3 h. After cooling, the mixture was treated with cold water and filtered. The solid obtained was then washed and dried. The crude product was recrystallized from ethanol to give **2** as yellow crystals, yield 49%; ^{1}H NMR (400 MHz, DMSO-d_6/TMS) δ: 1.42 (s, 36H, $12 \times CH_3$), 3.05 (s, 4H, $2 \times CH_2$), 7.37 (s, 2H, OH), 7.44 (s, 4H, Ar-H), 7.52 (s, 2H, $2 \times {=}CH{-}$). IR (KBr) ν: 3611, 3406, 1665, 1619, 1588, 1424, 1322, 1255, 1184, 1127, 1009, 943, 876, 774, 605, 492 cm^{-1}. MS m/z: 517 (M + 1). Anal. calcd for $C_{35}H_{48}O_3$: C 81.35, H 9.36; found: C 81.12, H 9.23.

2.2.3. 2,5-Bis-(9-anthrylmethylidene)cyclopentanone (3)

This compound was prepared according to the procedure described for **1**, from 20 mmol 9-anthrylaldehyde and 10 mmol cyclopentanone. Red crystals, yield 56%, mp > 235 °C; ^{1}H NMR (500 MHz, $CDCl_3$/TMS) δ: 2.30 (s, 4H, $2 \times CH_2$), 7.48–7.54 (m, 8H, Ar-H), 8.01–8.12 (m, 8H, Ar-H), 8.47 (s, 2H, Ar-H), 8.59 (s, 2H, $2 \times {=}CH{-}$). IR (KBr) ν: 1676, 1634, 1627, 1441, 1408, 1359, 1310, 1207, 1157, 1089, 956, 890, 847, 796, 735, 728, 535, 512 cm^{-1}. MS m/z: 461.00 (M + 1). Anal. calcd for $C_{35}H_{24}O$: C 91.27, H 5.25; found: C 91.53, H 5.18.

2.3. X-ray crystallography

Suitable single crystals of **1**, **2** and **3** for X-ray structural analysis were obtained by evaporation of ethanol or DMF

Table 1
Crystal data and structure refinement.

Compound	**1**	**2**	**3**
Empirical formula	$C_{31}H_{24}O_3$	$C_{35}H_{48}O_3 \cdot C_2H_6O$	$C_{35}H_{24}O \cdot C_3H_7NO$
Formula weight	444.50	562.80	533.64
Temperature (K)	293 (2)	273 (2)	273 (2)
Crystal system	Monoclinic	Monoclinic	Triclinic
Space group	$P2_1/c$	$P2_1/c$	$P\bar{1}$
Unit cell dimensions			
a (nm)	0.61260 (12)	1.0812 (17)	1.05631 (15)
b (nm)	4.3862 (9)	1.878 (3)	1.10456 (15)
c (nm)	0.85740 (17)	1.895 (3)	1.36961 (19)
α (°)	90	90	98.092 (2)
β (°)	97.20 (3)	99.55 (3)	90.018 (3)
γ (°)	90	90	115.825 (3)
Volume (nm^3), Z	2.2857 (8), 4	3.794 (10), 4	1.4207 (3), 2
D_{calc} (Mg/m^3)	1.292	0.985	1.247
Absorption coefficient (mm^{-1})	0.082	0.062	0.076
F (0 0 0)	936	1232	564
Crystal size (mm)	0.30 × 0.20 × 0.10	0.21 × 0.16 × 0.12	0.20 × 0.15 × 0.11
θ range for data collection (°)	1.86–25.33	1.54–25.05	1.51–25.05
Limiting indices	$-7 \le h \le 7$ $0 \le k \le 52$ $0 \le l \le 10$	$-12 \le h \le 11$ $-17 \le k \le 22$ $-20 \le l \le 22$	$-12 \le h \le 12$ $-12 \le k \le 13$ $-16 \le l \le 16$
Reflections collected/unique	4503/4132 [$R_{int} = 0.0509$]	16162/6478 [$R_{int} = 0.0723$]	7592/5009 [$R_{int} = 0.0270$]
Max. and min. transmission	0.9918 and 0.9758	0.9926 and 0.9871	0.9917 and 0.9849
Data/restraints/ parameters	4132/147/307	6478/1/374	5009/0/371
Goodness-of-fit on F^2	1.002	1.009	1.010
Final R indices [$I > 2$ sigma (I)]	$R_1 = 0.0878$ $wR_2 = 0.1532$	$R_1 = 0.0643$ $wR_2 = 0.1463$	$R_1 = 0.0576$ $wR_2 = 0.1411$
R indices (all data)	$R_1 = 0.1864$ $wR_2 = 0.1897$	$R_1 = 0.1614$ $wR_2 = 0.1917$	$R_1 = 0.1092$ $wR_2 = 0.1734$
Extinction coefficient		0.0035 (7)	0.0059 (19)
Largest diff. peak and hole (e.nm^{-3})	240 and 207	214 and 175	240 and 203
CCDC	750903	750906	750902

solution. The diffraction data for three structures were collected with a Enraf-Nonius CAD-4 diffractometer or Bruker Smart Apex 1000 CCD area detector using a graphite monochromated Mo Kα radiation ($\lambda = 0.071073$ nm) at 293 (2) K or 273 (2) K. The structures were solved by direct methods with SHELXS-97 program and refinements on F^2 were performed with SHELXL-97 program by full-matrix least-squares techniques with anisotropic thermal parameters for the non-hydrogen atoms. All H atoms were initially located in a difference Fourier map. The methyl H atoms were then constrained to an ideal geometry, with C–H = 0.096 nm and $U_{iso}(H) = 1.5U_{eq}(C)$. The hydroxyl H atom was treated as a riding atom, with O–H = 0.082 nm and $U_{iso}(H) = 1.5U_{eq}(O)$. All other H atoms were placed in geometrically idealized positions and constrained to ride on their parent atoms with C–H distances 0.093–0.097 nm and $U_{iso}(H) = 1.2U_{eq}(C)$. A summary of the crystallographic data and structure refinement details is given in Table 1.

3. Results and discussion

3.1. Synthesis

Derivatives of bis(arylmethylidene) cyclopentanone are usually obtained by the Claisen–Schmidt condensation. The properly substituted arylaldehydes were reacted with cyclopentanone in the presence of sodium hydroxide, to afford bis(benzylidene) cyclopentanone derivatives **1** and **3** in 56–67% yields. On the other hand, although compound **2** has been studied previously by other groups [24,25], the crystal structure of **2** has not been reported. So, with a modified method, we prepared the **2** by reaction of 3,5-di-tert-butyl-4-hydroxybenzaldehyde with cyclopentanone in the presence of concentrated sulfuric acid in methanol under reflux. Compared with the method reported in literature [24,25], such a modified procedure for preparation of compound **2** affords the advantage of short reaction time.

Concerning stereochemistry, the olefinic bis(arylmethylidene) cyclopentanones were obtained in *E*-configuration for sterical reasons since in the *Z*-isomers the aryl rings have to turn out of the plane of the olefinic double bond because of interaction of the *ortho* H atoms with the carbonyl O-atom. Also, the *E*-configuration of the olefinic bond of **1**, **2** and **3** was established by X-ray diffraction crystal structure analysis in this work.

All the synthesized compounds have been characterized on the basis of their physical data and spectral analysis. The IR spectra of these compounds showed two strong bands at 1665–1685 and 1619–1634 cm^{-1} due to C=O and C=C double bond, respectively, indicating the formation of arylmethylidenecyclopentanone backbone. In the IR spectra of **2**, the ν(O–H) vibrations occur as very strong absorption at 3611 and 3406 cm^{-1}. All the compounds show the NMR signals for different kinds of protons at their respective positions. The values are consistent with their predicted structures. The complete chemical shifts for all compounds are listed in Experimental part.

3.2. Crystal structure

X-ray diffraction crystal structure analysis reveals that the three molecules, **1**, **2** and **3**, are remarkably similar. All three are adopt an *E*-configuration about the central olefinic bonds, exhibiting a butterfly-shaped geometry, which is similar to that of **TMPCP** [26], as shown in Fig. 3–10. Both compound **1** and **2** crystallized monoclinically with space group $P2_1/c$, while compound **3** crystallized in the triclinic $P\bar{1}$ space group.

In compound **1** (Fig. 3), the central cyclopentanone ring is essentially planar. And the cyclopentanone ring, the olefinic bonds

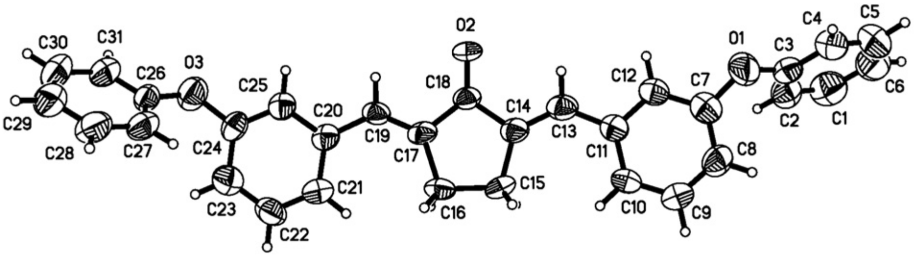

Fig. 3. The molecular structure of **1**, showing the atom-labelling scheme. Displacement ellipsoids are drawn at the 50% probability level. H atoms are shown as small spheres of arbitrary radius.

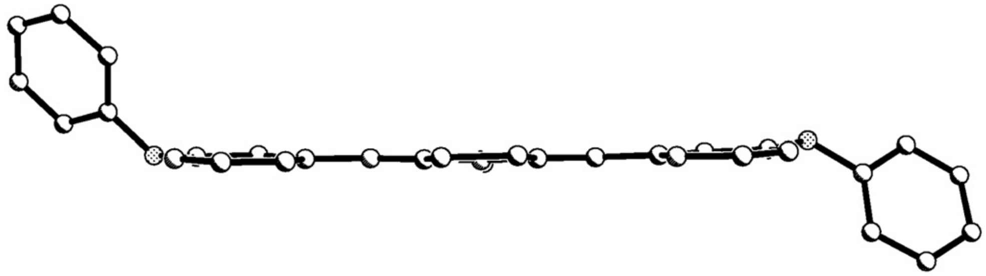

Fig. 4. The side elevation of **1**. H atoms are omitted for clarity.

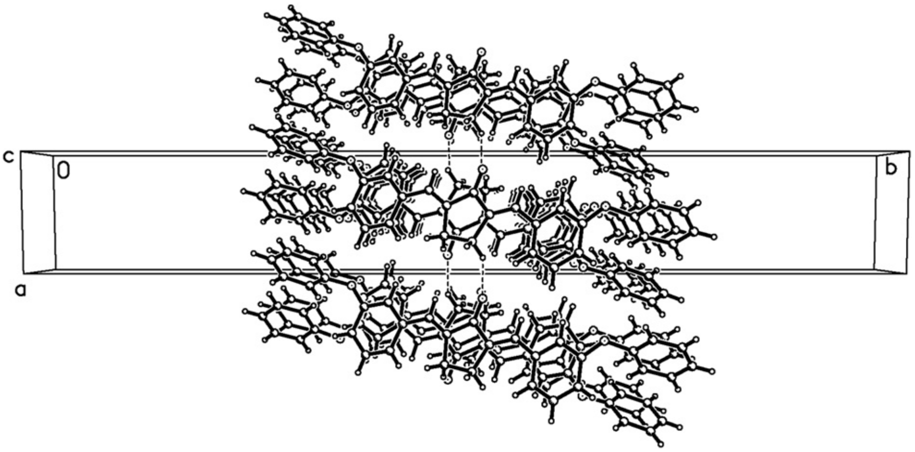

Fig. 5. A packing diagram for **1**, viewed down the *c* axis. The dashed lines indicate hydrogen bonds.

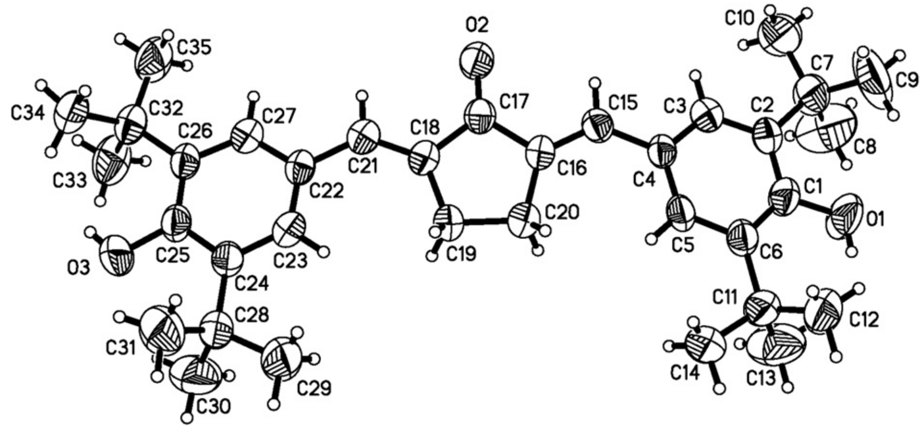

Fig. 6. The molecular structure of **2**, showing the atom-labelling scheme. Displacement ellipsoids are drawn at the 50% probability level. H atoms are shown as small spheres of arbitrary radius. Ethanol molecule is omitted for clarity.

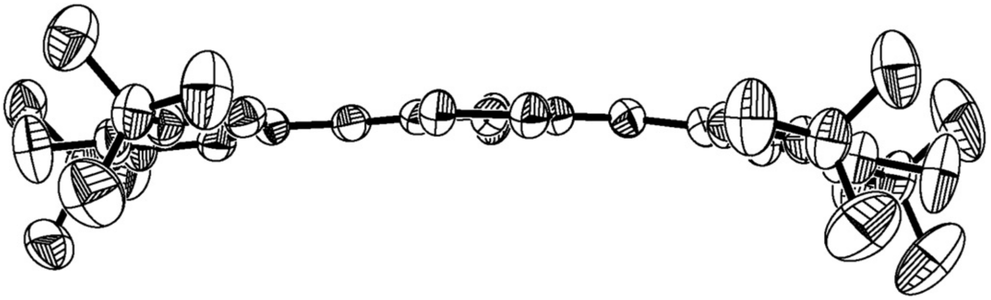

Fig. 7. The side elevation of **2**. Ethanol molecule and H atoms are omitted for clarity.

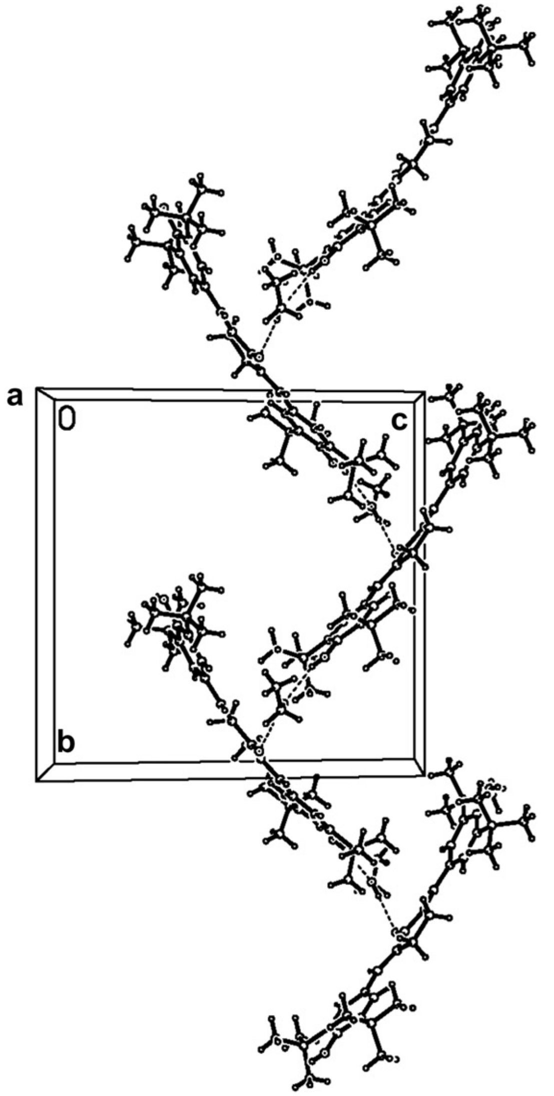

Fig. 8. The chain structure formed *via* hydrogen bonds in **2**. The dashed lines indicate hydrogen bonds.

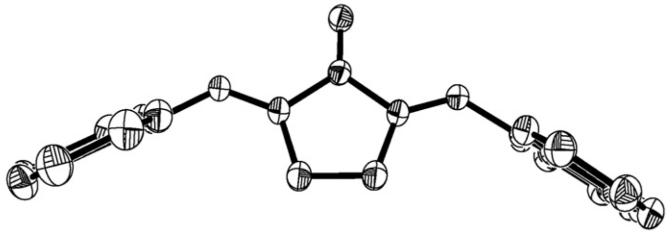

Fig. 10. The side elevation of 3. DMF molecule and H atoms are omitted for clarity.

and the two phenyl rings (C7–C12 and C20–C25) are almost coplanar [r.m.s. deviation = 0.01373 nm, maximum deviation = 0.0099 nm for atom C18], which allows conjugation. However, the two terminal phenyl rings (C1–C6 and C26–C31) make a dihedral angle of 65.5°, and are twisted out of the plane of the central cyclopentanone unit on the two sides. The dihedral angles between the cyclopentanone ring plane and the C1–C6 and C26–C31 phenyl ring planes are 68.5 and 62.6°, respectively. Therefore, apart from the two phenyl rings (C1–C6 and C26–C31), the rest of the molecule is nearly coplanar (Fig. 4).

The molecules are linked together by weak intermolecular C–H…O (C15–H15B…O2: C–H = 0.097 nm, H15B…O2 = 0.25 nm, C15…O2 = 0.3339 (5) nm, C15–H15B…O2 = 147°) hydrogen bonds into a one-dimensional chain along the *a*-axis. The molecules are assembled to form a layer structure (Fig. 5).

The molecule structure of **2** is shown in Fig. 6. Like molecule **1**, in **2** also, the central cyclopentanone ring is planar. The dihedral angles between the cyclopentanone ring plane and the C1–C6 and C22–C27 phenyl ring planes are 13.1 and 11.3°, respectively. Therefore, apart from the terminal methyl groups, the rest of the molecule exhibits a bent planar configuration, as observed in Fig. 7.

In addition, of the twelve methyl groups C10, C14, C29 and C35 are coplanar with one of the benzene rings, with the others showing out-of-plane twists ranging from ~59.3 to 64.5°.

The molecules are linked into a *zigzag* one-dimensional chain along the *b*-axis by intermolecular O–H…O (O3–H3…O4: O–H = 0.082 nm, H3…O4 = 0.24 nm, O3…O4 = 0.2974 (5) nm, O3–H3…O4 = 131°; O4–H4…O2$^{\mathrm{i}}$: O–H = 0.082 nm, H4…O2 = 0.21 nm, O4…O2 = 0.2968 (5) nm, O4–H4…O2 = 178°, symmetry

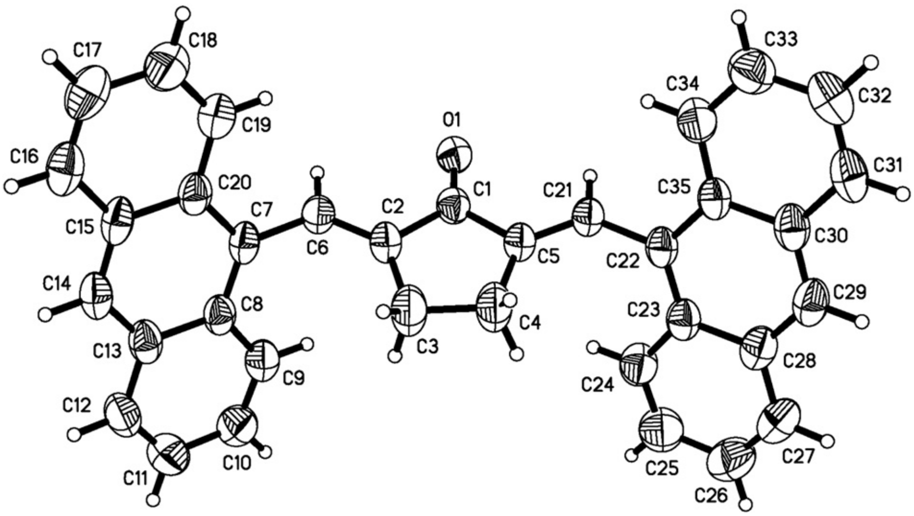

Fig. 9. The molecular structure of **3**, showing the atom-labelling scheme. Displacement ellipsoids are drawn at the 50% probability level. H atoms are shown as small spheres of arbitrary radius. DMF molecule is omitted for clarity.

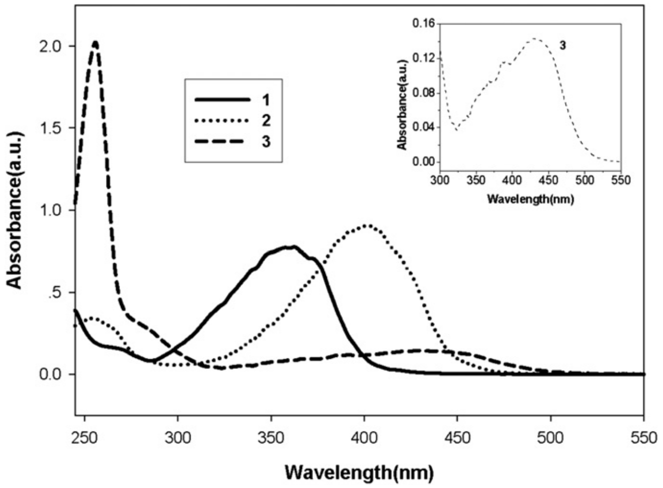

Fig. 11. Absorption spectra of the bis(arylmethylidene)cyclopentanones in chloroform solution. The inset shows an expansion of the 430 nm absorption peak of **3**.

code: (i) $-x+2$, $y-1/2$, $-z+1/2$) hydrogen bonds (Fig. 8). The ethanol molecule plays a significant role in the crystal packing as it is the acceptor in one hydrogen bond and a donor in another.

The compound **3** formed crystalline clathrates with DMF in a 1:1 molar ratio. As can be seen from Fig. 9, in **3**, the central cyclopentanone ring is essentially planar, while the two anthracene rings (C7–C20 and C22–C35) is rotated significantly out of the plane of the central cyclopentanone unit (Fig. 10), and make a dihedral angle of 57.6°. The dihedral angles between the cyclopentanone ring plane and the C7–C20 and C22–C35 anthracene ring planes are 67.3 and 61.8°, respectively. As a result, the whole compound is not a planar molecule. Similar geometry has been observed in related anthracene analogues, which were reported previously [27]. But these structural characteristics of compound **3** are remarkably different from those of in **1** and **2**. Comparison with **1** and **2** suggests that the anthracene system caused a significantly rotation relative to the substituted phenyl system, owing to the larger steric effect of the anthracene ring. In addition, the crystal packing of **3** is stabilized by weak intermolecular hydrogen bonds and π–π stacking interactions.

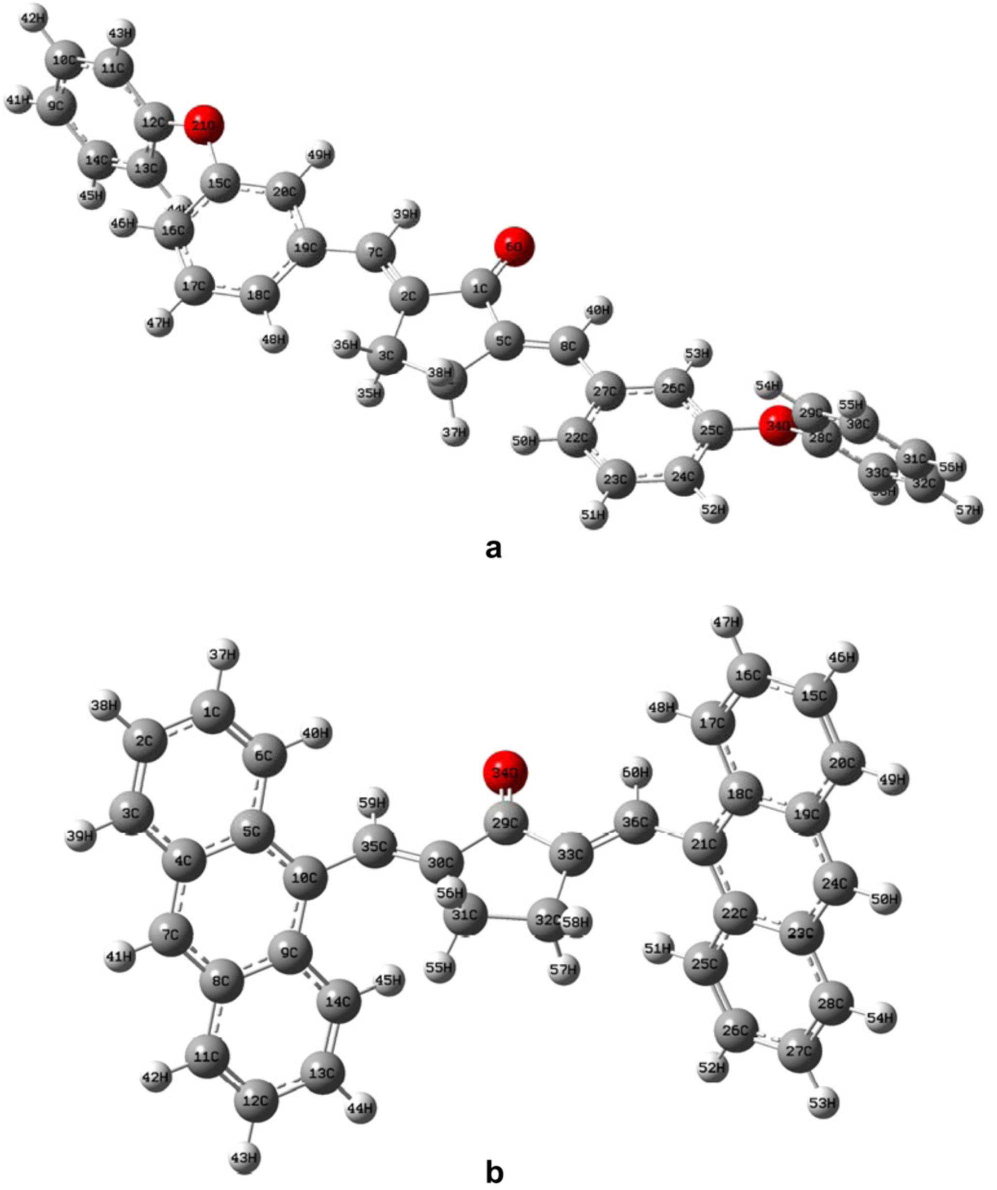

Fig. 12. Optimized structures of (*a*) **1** and (*b*) **3** by DFT method.

3.3. Absorption spectra

The structures of the target molecules are shown in Fig. 2. These molecules consist of a typical $D-\pi-A-\pi-D$ structure, where the substituted phenyl or anthryl, vinyl and carbonyl groups are employed as donor (D), π-conjugated center (π) and acceptor (A) moieties, respectively. Moreover, such a structural modification could be expected to result in notable changes in the π-conjugated length and red shifts in the absorption spectra.

UV–vis absorption spectra of these molecules in diluted chloroform solutions (2×10^{-5} M) are given in Fig. 11. It can be seen from Fig. 11 that, the compounds comprise two bands in the wavelength range from 250 to 550 nm, while almost no linear absorption was observed beyond 550 nm. The bands at shorter wavelength (250–280 nm) are due to localized $\pi-\pi^*$ transition of the phenyl and anthryl moieties, while the longer wavelength bands with λ_{max} ranging from 362 to 430 nm can be assigned to the intramolecular charge-transfer transitions involving the whole electronic system of the compounds with a considerable charge-transfer character originating mainly from the substituted phenyl or anthryl moiety and pointing towards the carbonyl group. And, the maximum absorption peaks of the first absorption band of the target molecules are red-shifted from **1** ($\lambda_{max} = 362$ nm, $\varepsilon = 3.87 \times 10^4$ L mol^{-1} cm^{-1}) to **2** ($\lambda_{max} = 402$ nm, $\varepsilon = 4.52 \times 10^4$ L mol^{-1} cm^{-1}), and to **3** ($\lambda_{max} = 430$ nm, $\varepsilon = 7.18 \times 10^3$ L mol^{-1} cm^{-1}). Obviously, the anthracene system caused a bathochromic effect of approximately 28–68 nm relative to the substituted phenyl system. The results above imply that more π-electrons and longer π-conjugated structure may be involved in **3** than those in other. As a result, the red shift of absorption can possibly occur. Additionally, it could be recognized that the absorption band of **2** exhibited a red-shift of 40 nm compared to that of **1**. This difference might be attributed to the stronger electron-donating effect of hydroxy group.

3.4. Quantum chemical calculations

The geometry structures of **1** and **3** were optimized with density function theory (DFT) at the B3LYP/6-31G level, all structure optimizations and energy calculations were performed with the GAUSSIAN 98 program. Their structure parameters and energy of frontier molecular orbital were obtained. The optimal structures of **1** and **3** are depicted in Fig. 12. The HOMO (highest occupied molecular orbital) and LUMO (lowest unoccupied molecular orbital) levels of **1** and **3** are shown in Figs. 13 and 14.

It was found that the B3LYP/6-31G optimized structures of **1** and **3** (Fig. 12) are in good agreement with the X-ray crystallographic data. Therefore, the results using DTF at B3LYP/6-31G level is creditable.

Generally, the energy values of LUMO and HOMO and their energy gap reflect the chemical activity of the molecule. HOMO as an electron donor represents the ability to donate an electron, while LUMO as an electron acceptor represents the ability to obtain an electron. The smaller the LUMO and HOMO energy gaps, the easier it is for the HOMO electrons to be excited [28].

Figs. 13 and 14 show the frontier orbitals of the molecules. Based on the calculations, the electron cloud of HOMO for compound **1** is mainly focused on four benzene rings, which is composed of $\pi-\pi$ orbits from C–C. Compared with HOMO, the electron cloud on the central cyclopentanone of LUMO increases clearly, especially on carbonyl group (Fig. 13). The above suggests that electrons transfer from benzene ring to carbonyl group to some extent. Similarly, for compound **3**, the electron cloud of HOMO is focused on two anchracene rings. Also, the electron cloud on the central cyclopentanone of LUMO increases clearly (Fig. 14). Therefore, when electrons transfer from HOMO to LUMO, the electron cloud density on cyclopentanone increases, indicating that electrons transfer from benzene or anchracene rings to cyclopentanone.

The energies of the HOMO and LUMO for compound **1** based on the optimized structure were computed at −5.91 and −2.27 eV, respectively. Similarly, the energies of the HOMO and LUMO of compound **3** are −5.22 and −2.29 eV, respectively. Obviously, the LUMO energy of **3** is slight lower than that of compound **1**, and the energy gap of **3** is smaller than that of **1**. But the HOMO energy of compound **3** is higher than that of compound **1**. Consequently, the electrons transfer from HOMO to LUMO in **3** is relatively easier than that in **1**. Furthermore, we noticed that the presence of anthracene makes the HOMO rather high in energy and decrease the energy gap between HOMO and LUMO. So, compared to **1**, a bathochromic shift of **3** can be observed in the electron absorption spectrum. These results are quite consistent with those from the experiment

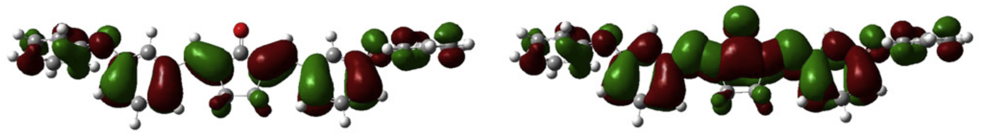

HOMO(117) $E = -5.91$ **eV** **LUMO(118)** $E = -2.27$ **eV**

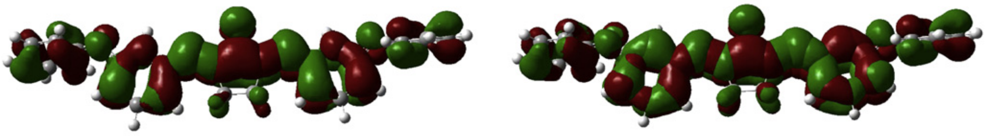

HOMO-1(116) $E = -6.01$ **eV** **LUMO+1(119)** $E = -0.94$ **eV**

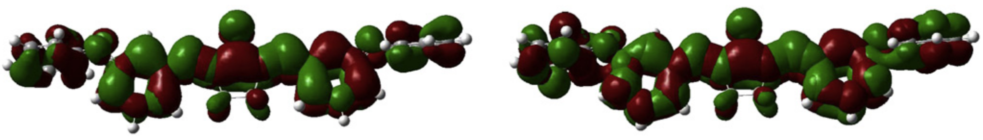

HOMO-2(115) $E = -6.24$ **eV** **LUMO+2(120)** $E = -0.28$ **eV**

Fig. 13. Molecular orbital surface and energies of the main frontier molecular orbitals for **1**.

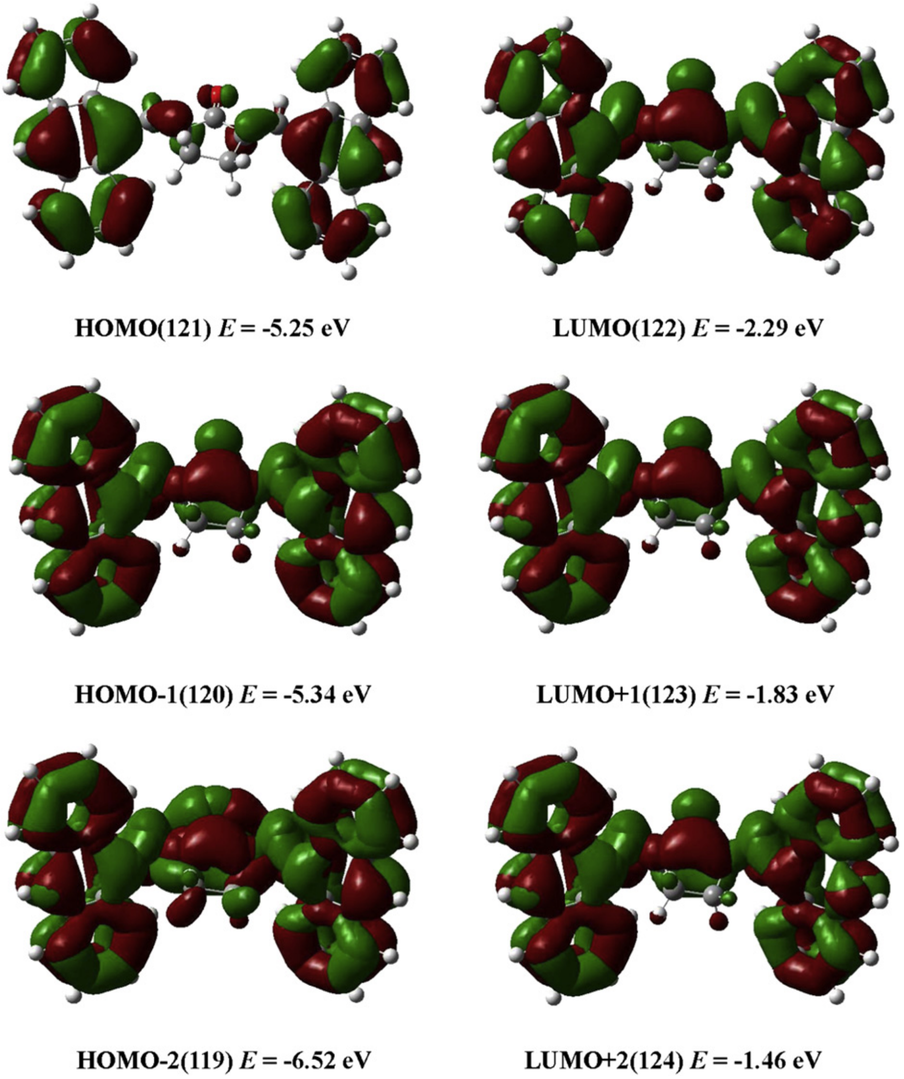

Fig. 14. Molecular orbital surface and energies of the main frontier molecular orbitals for **3**.

in this work. In addition, we also found a pair of doublet split in energy, HOMO-1 and HOMO-2.

In all, the different substituents on cyclopentanone derivatives can affect the energy and gap of frontier molecular orbital greatly, which provide reference for the molecular design and energy gap adjustment.

4. Conclusions

The synthesis, characterization and crystal structures determined by single-crystal X-ray diffraction, of three bis(arylmethylidene) cyclopentanone dyes, **1**, **2** and **3**, are reported. The absorption spectra of these three molecules were discussed. With the anchracene moiety, the edge of absorption spectra of **3** was shift to long wavelength side. The molecular structures of **1** and **3** were optimized using density function theory (DFT) at B3LYP/6-31G level while the HOMO and LUMO levels of **1** and **3** were deduced.

Supplementary material

The crystallographic data (excluding structure factors) of **1**, **2** and **3** have been deposited with the Cambridge Crystallographic Center as supplementary publication no. CCDC 750903, 750906 and 750902. Copy of this information may be obtained free of charge via www: http://www.ccdc.cam.ac.uk or from The Director, CCDC, 12 Union Road, Cambridge CB221EZ, UK (fax: +44 1223/336 033; email: deposite@ccdc.cam.ac.uk). Structural factors are available on request from the authors.

Acknowledgements

This project was supported by the National Natural Science Foundation of China (No. 60877024) and the Foundation of Taishan University (No. Y04-2-02).

References

[1] Shao WY, Cao YN, Yu ZW, Pan WJ, Qiu X, Bu XZ, et al. Facile preparation of new unsymmetrical curcumin derivatives by solid-phase synthesis strategy. Tetrahedron Letters 2006;47:4085–9.
[2] Liang G, Yang SL, Liang LJ, Zao Y, Shao LL, Xiao J, et al. Synthesis and antibacterial properties of mono-carbonyl analogues of curcumin. Chemical & Pharmaceutical Bulletin 2008;56:162–7.
[3] Gafner S, Lee SK, Cuendet M, Barthelemy S, Vergnes L, Labidalle S, et al. Biologic evaluation of curcumin and structural derivatives in cancer chemoprevention model systems. Phytochemistry 2004;65:2849–59.

[4] Robinson TP, Hubbard RB, Ehlers TJ, Arbiser JL, Goldsmith DJ, Bowen JP. Synthesis and biological evaluation of aromatic enones related to curcumin. Bioorganic & Medicinal Chemistry 2005;13:4007–13.

[5] Zambre AP, Kulkarni VM, Padhye S, Sandur SK, Aggarwal BB. Novel curcumin analogs targeting TNF-induced NF-kappa B activation and proliferation in human leukemic KBM-5 cells. Bioorganic & Medicinal Chemistry 2006;14:7196–204.

[6] Bhagat S, Sharma R, Chakraborti AK. Dual-activation protocol for tandem cross-aldol condensation: an easy and highly efficient synthesis of α,α'-bis(aryl/alkylmethylidene)ketones. Journal of Molecular Catalysis A: Chemical 2006;260:235–40.

[7] Juang SH, Pan WY, Kuo CC, Liou JP, Hung YM, Chen LT, et al. A novel bis-benzylidenecyclopentanone derivative, BPR0Y007, inducing a rapid caspase activation involving upregulation of Fas (CD95/APO-1) and wild-type p53 in human oral epidermoid carcinoma cells. Biochemical Pharmacology 2004;68:293–303.

[8] Santo RD, Costi R, Artico M, Tramontano E, Colla PL, Pani A. HIV-1 integrase inhibitors that block HIV-1 replication in infected cells. Planning synthetic derivatives from natural products. Pure and Applied Chemistry 2003;75:195–206.

[9] Handler N, Jaeger W, Puschacher H, Leisser K, Erker T. Synthesis of novel curcumin analogues and their evaluation as selective cyclooxygenase-1 (COX-1) inhibitors. Chemical & Pharmaceutical Bulletin 2007;55:64–71.

[10] Youssef KM, El-Sherbeny MA. Synthesis and antitumor activity of some curcumin analogs. Archiv der Pharmazie – Chemistry in Life Sciences 2005;338:181–9.

[11] Robinson TP, Ehlers TE, Hubbard RB, Bai XH, Arbiser JL, Goldsmith DJ, et al. Design, synthesis, and biological evaluation of angiogenesis inhibitors: aromatic enone and dienone analogues of curcumin. Bioorganic & Medicinal Chemistry Letters 2003;13:115–7.

[12] Costi R, Santo RD, Artico M, Massa S, Ragno R, Loddo R, et al. 2,6-Bis(3,4,5-trihydroxybenzylydene) derivatives of cyclohexanone: novel potent HIV-1 integrase inhibitors that prevent HIV-1 multiplication in cell-based assays. Bioorganic & Medicinal Chemistry 2004;12:199–215.

[13] Liang G, Yang SL, Zhou HP, Shao LL, Huang KX, Xiao J, et al. Synthesis, crystal structure and anti-inflammatory properties of curcumin analogues. European Journal of Medicinal Chemistry 2009;44:915–9.

[14] Nugroho AE, Ikawati Z, Sardjiman Maeyama K. Effects of benzylidenecyclopentanone analogues of curcumin on histamine release from mast cells. Biological & Pharmaceutical Bulletin 2009;32:842–9.

[15] Das U, Kawase M, Sakagami H, Ideo A, Shimada J, Molnar J, et al. 3-(3,4,5-Trimethoxyphenyl)-1-oxo-2-propene: a novel pharmacophore displaying potent multidrug resistance reversal and selective cytotoxicity. Bioorganic & Medicinal Chemistry 2007;15:3373–80.

[16] Pivovarenko VG, Klueva AV, Doroshenko AO, Demchenko AP. Bands separation in fluorescence spectra of ketocyanine dyes: evidence for their complex formation with monohydric alcohols. Chemical Physics Letters 2000;325:389–98.

[17] Doroshenko AO, Grigorovich AV, Posokhov E, Pivovarenko VG, Demchenko AP. Bis-azacrown derivative of di-benzilidene-cyclopentanone as alkali earth ion chelating probe: spectroscopic properties, proton accepting ability and complex formation with Mg^{2+} and Ba^{2+} ions. Molecular Engineering 1999;8:199–215.

[18] Doroshenko AO, Sychevskaya LB, Grygorovych AV, Pivovarenko VG. Fluorescence probing of cell membranes with azacrown substituted ketocyanine dyes. Journal of Fluorescence 2002;12:455–64.

[19] Yamashita K, Imahashi S, Ito S. Synthesis of benzylideneketone dyes and their photochemical properties as a sensitizer for alkali-developable photopolymerization systems. Dyes and Pigments 2008;76:748–53.

[20] Xue JQ, Zhao YX, Wu J, Wu FP. Novel benzylidene cyclopentanone dyes for two-photon photopolymerization. Journal of Photochemistry and Photobiology A: Chemistry 2008;195:261–6.

[21] Wu J, Shi MQ, Zhao YX, Wu FP. Two-photon absorption property and photopolymerization sensitizing efficiency of asymmetrical benzylidene cyclopentanone dyes. Dyes and Pigments 2008;76:690–5.

[22] Raj AA, Raghunathan R, Kumari MRS, Raman N. Synthesis, antimicrobial and antifungal activity of a new class of spiro pyrrolidines. Bioorganic & Medicinal Chemistry 2003;11:407–19.

[23] Amarasekara AS. Nitrosation of β'-hydroxylamino-α,β-unsaturated oximes: synthesis of 1,7-dioxa-2,6-diaza-spiro[4,4]nona-2,8-diene ring system. Tetrahedron Letters 2005;46:2635–8.

[24] Du ZY, Liu RR, Shao WY, Mao XP, Ma L, Gu LQ, et al. α-Glucosidase inhibition of natural curcuminoids and curcumin analogs. European Journal of Medicinal Chemistry 2006;41:213–8.

[25] Sardjiman SS, Reksohadiprodjo MS, Hakim L, van der Goot H, Timmerman H. 1,5-Diphenyl-1,4-pentadiene-3-ones and cyclic analogues as antioxidative agents. synthesis and structure–activity relationship. European Journal of Medicinal Chemistry 1997;32:625–30.

[26] Sun YF, Liu Y, Zhang FY, Chen HJ, Cui YP. (2E,5E)-2,5-Bis(3,4,5-trimethoxybenzylidene)cyclopentanone. Acta Crystallographica Section E: Structure Reports Online 2008;64:o1964.

[27] Sun YF, Zheng DD, Ma CL. Synthesis and crystal structure of 3-(3-anthracen-9-yl-acryloyl)-6,8-di-tert-butylcoumarin. Analytical Sciences: X-ray Structure Analysis Online 2005;21:X177–8.

[28] Riahi S, Eynollahi S, Ganjali MR. Calculation of standard electrode potential and study of solvent effect on electronic parameters of anthraquinone-1-carboxylic Acid. International Journal of Electrochemical Science 2009;4:1128–37.